Desalination and Water Treatment
www.deswater.com

doi: 10.5004/dwt.2020.25369

184 (2020) 214–224
April

Isotherm, kinetics and thermodynamic parameters study of arsenic (III) and copper (II) adsorption onto *Limonia acidissima* shell carbon

Virender Yadav[a,*], D.P. Tiwari[a,b], Mamta Bhagat[a]

[a]*Department of Chemical Engineering, Deenbandhu Chottu Ram University of Science and Technology, Murthal, Sonipat-131001, Haryana, India, emails: virenderydv@gmail.com (V. Yadav), dptiwari3@gmail.com (D.P. Tiwari), mamtabhagatduper@gmail.com (M. Bhagat)*
[b]*Rajiv Gandhi Government Engineering College, Nagrota Bagwan Taluka, Kangra-176047 Himachal Pradesh, India*

Received 7 April 2019; Accepted 22 December 2019

ABSTRACT

The adsorption of heavy metal ions As(III) and Cu(II) from aqueous solution on activated carbon prepared from *Limonia acidissima* shell was studied in batch mode. Different characterization of *Limonia acidissima* shell carbon was carried out using Fourier transform infrared spectroscopy, X-ray diffraction, scanning electron microscopy, and Brunauer–Emmett–Teller. The effects of various parameters such as contact time, initial heavy metal concentration, and dosage of *Limonia acidissima* shell carbon were investigated. The process optimization of mentioned parameters was also intended, and it was observed that around 92.2% of As(III) and 84.1% Cu(II) ions were removed with 50 mg of *Limonia acidissima* shell carbon at 303 K with 180 min. The adsorption kinetic studies showed that the adsorption follows the pseudo-second-order model for both As(III) and Cu(II). The equilibrium data were analyzed using Langmuir, Freundlich, Temkin, and D-R adsorption isotherm models. The adsorption of As(III) and Cu(II) in single solution followed the Langmuir isotherm model. The maximum adsorption capacities of *Limonia acidissima* carbon for As(III) and Cu(II) were 68.77 and 76.92 mg/g, respectively. The positive enthalpy change for adsorption of As(III) and Cu(II) on *Limonia acidissima* shell carbon confirms the endothermic nature of adsorption while Gibbs's free energy change confirms the spontaneity of the process.

Keywords: Arsenic; Copper; Activated carbon; *Limonia acidissima* shell; Wastewater treatment

1. Introduction

Contamination of heavy metals such as arsenic, copper, etc. in drinking water and underground water has created serious water pollution in Asian developing countries such as India, Nepal, and other parts of the world [1]. These types of water pollutants are non-biodegradable, toxic in nature, and have adverse effects on human health [2]. These heavy metals cause serious health effects, including skin manifestations, visceral cancers, vascular disease, organ damage, nervous system damage, liver damage, Wilson disease, and insomnia [3]. The accumulation of heavy metals in water bodies due to various industries such as mining industry, electric and electronic manufacturing industry, glass manufacturing industry, wood preservative industries, production of paints and pigments, automobiles industries, etc. [4]. Research curiosity into the adsorption process based on low-cost adsorbents to substitute costly wastewater treatment methods such as chemical precipitation, ion-exchange, electro-flotation, membrane separation, electro-dialysis, solvent extraction, advanced oxidation processes, etc. is attracting concerns of scientists [5]. The adsorption process is a powerful technology which has been found to be effective in removing heavy metals from domestic and industrial

---

* Corresponding author.

wastewater [6]. Various low-cost adsorbents derived from agricultural waste such as maize cob and husk [7], orange peel [8], pecan shells activated carbon [9], rice husk [10], coconut shell charcoal [11], modified rice hull [12], pine cone activated carbon [13], hazelnut shell activated carbon [14], green vegetable-derived activated carbon [15], *Phaseolus aurens* hulls derived activated carbon [16], pyrolysed hardwood and corn straw [17], *Polygonum orientale* Linn. derived activated carbon [18], activated carbon from bagasse [19], modified *Dalbergia sissoo* pods [20], *Eucalyptus bark* [21], biochar prepared from *Pistachio green* hulls [22], sodium carbonate treated rice husk [23], activated carbon from *Cucumis melo* peel [24], chemically modified *Kigelia africana* [25], seed cake powder, sesame seed cake powder and coconut cake powder [26], and *Padina gymnospora* residue [27] have been used for adsorptive removal of heavy metals. In this paper, we focus on the preparation of activated carbons from *Limonia acidissima* shell using sulfuric acid (H_2SO_4) as an activating agent. Sulfuric acid is more suitable than zinc chloride because it is inexpensive, nonvolatile and the less hazardous as compared with zinc compounds [28,29]. The objective of this study is to investigate adsorption characteristics of As(III) and Cu(II) from aqueous solution onto activated carbon derived from *Limonia acidissima* shell. *Limonia acidissima* shell is a potential biomass for production of activated carbon due to its high fixed carbon and low ash content. The study of various equilibrium adsorption operations, such as initial concentration, contact time and pH, various isotherm models and adsorption kinetic models provide basic information required for the design and operation of adsorption equipments for wastewater treatment. The various thermodynamic parameters were also investigated which established the thermodynamic feasibility and the thermodynamic nature of As(III) and Cu(II) adsorption on *Limonia acidissima* shell carbon.

2. Materials and methods

2.1. Activated carbon preparation

The *Limonia acidissima* shell was collected from Deenbandhu Chhotu Ram University of Science and Technology Murthal, Sonipat campus and Karnal (India). The outer shell of *Limonia acidissima* was cut into small pieces, followed by several washing with double distilled water to remove impurities and dust. Then it was air dried in sunlight for 10–15 d. The air dried *Limonia acidissima* shells were kept inside an oven at 60°C for 24 h for complete removal of moisture. The dried *Limonia acidissima* shells were crushed in a household grinder and sieved to 300 micron through a laboratory sieve shaker. The grounded *Limonia acidissima* shells were soaked with concentrated sulfuric acid (H_2SO_4) at 1:1 ratio (w/v). The slurry form of powder precursor was uniformly mixed and kept for 48 h for complete soaking of H_2SO_4 on grounded *Limonia acidissima* shells surface. The slurry was placed in a muffle furnace at 600°C for 2 h for activation. The activated carbon of *Limonia acidissima* shell was neutralized to pH 7 by repeatedly washing with double distilled water. The carbon obtained from *Limonia acidissima* shell was dried inside an oven at 105°C for 2 h and packed in an airtight round neck bottle for further use [30,31].

2.2. Characterization of Limonia acidissima shell carbons

The infrared spectrum of *Limonia acidissima* shell carbons was obtained by Fourier transform infrared spectroscopy (PerkinElmer Frontier-BSEN60825, USA). The surface morphology of the activated carbon of *Limonia acidissima* shell was characterized using a scanning electron microscope (JEOL-6380, Japan). The surface area was calculated by the Brunauer–Emmett–Teller equation using adsorption data in a relative pressure range from 0.018 to 0.3. The nitrogen-adsorption measurements of the prepared samples were analyzed on the Quanta Chrome Novae-2200 model, USA. X-ray diffraction (Rigaku Miniflex-600, Japan) analysis was done to elucidate the structure of activated carbons.

2.3. Experiments of adsorption

The batch adsorption experiments were carried out using As(III) and Cu(II) as adsorbates and *Limonia acidissima* shell carbons as an adsorbent. All chemicals were purchased from Sigma-Aldrich Corp. Ltd. (India) with 99% purities. These chemicals were of analytical grade. As(III) and Cu(II) stock solutions (1,000 mg/L) were prepared by dissolving 1.75 g and 4.0 g of $NaAsO_2$ and $CuSO_4{\cdot}5H_2O$, respectively, in 1,000 mL double distilled water and different As(III) and Cu(II) concentrations (50, 60, 70, 80, 90 and 100 mg/L) were made by dilution of the 1,000 mg/L stock solutions. The concentration of metals ions was determined by atomic absorption spectrophotometer (Agilent series – 200, USA) was analyzed. The experiments were also performed to analyze the effect of various parameters such as contact time (20–180 min.), pH (2–12), adsorbent dosage (5–50 mg) and temperature (20°C–60°C). All batch experiments were conducted using 50 mL of 50 mg/L initial concentration both metals ions with 50 mg of *Limonia acidissima* shell carbon shaking at 120 rpm by orbital shaker until reaching the equilibrium (3 h) of As(III) and Cu(II) onto *Limonia acidissima* shell carbon at room temperature (30°C). The pH of the solution was maintained by using 0.1 N NaOH and 0.1 N HCl.

The sorption capacity q_e (mg/g) at a given time and removal efficiency was calculated by using Eqs. (1) and (2), respectively.

$$q_e = \left(C_0 - C_e\right)\frac{V}{m} \tag{1}$$

$$\%\ \text{removal} = \frac{\left(C_0 - C_e\right)}{C_0} \times 100 \tag{2}$$

Here C_0 (mg/L) and C_e (mg/L) are the initial and equilibrium heavy metal ions concentration in the solution of As(III) and Cu(II), respectively, V (L) and m (mg) are the volumes of solution, and weight of *Limonia acidissima* shell carbons.

2.4. Equilibrium adsorption isotherm models

The equilibrium data are basic requirements to understand the mechanism of adsorption. As(III) and Cu(II) adsorption by *Limonia acidissima* shell carbon were analyzed using well-known adsorption isotherm models such as Langmuir, Freundlich, Temkin, Dubinin–Radushkevich, and Scatchard isotherms. The Langmuir isotherm assumes monolayer coverage of adsorbent and adsorption occurs over homogeneous active sites on the adsorbent (Langmuir 1916), which is represented as Eq. (3) in the linear form [32]:

$$\frac{C_e}{q_e} = \left(\frac{1}{K_L q_m} + \frac{C_e}{q_m}\right) \tag{3}$$

The essential characteristic or feasibility of adsorption of the Langmuir isotherm is numerically expressed through separation factor (R_L) a dimensionless constant and can be calculated by using Eq. (4)

$$R_L = \frac{1}{\left(1 + K_L C_0\right)} \tag{4}$$

Here K_L (L/mg), C_0 and C_e are the Langmuir isotherm constant, initial and equilibrium concentration (both in mg/L) of As(III) and Cu(II) respectively. q_e (mg/g) represents the adsorbent capacity at equilibrium. The plot C_e/q_e vs. C_e gives the value q_m and K_L.

The Freundlich isotherm model is generally applicable on the heterogeneous surface for multilayer adsorption. The linear form is given below:

$$\log q_e = \log K_f + \frac{1}{n}\log C_e \tag{5}$$

Here K_f (mg/g) adsorption capacity and $1/n$ adsorption intensity were found with plot log q_e vs. log C_e [33]. n, which is greater than 1, shows that the adsorption isotherm is favorable [34].

Temkin isotherm model justifies the heat of adsorption for all molecules layers, which decrease linearly with the coverage involved in this interaction. The Temkin isotherm is expressed in Eq. (6):

$$q_e = B \ln A_T + B \ln C_e \tag{6}$$

A_T (L/mol) and B are equilibrium binding energy and heat of the adsorption obtained from intercept and slope of the graph between q_e vs. ln C_e.

Dubinin–Radushkevich isotherm model is selected for the estimation of characteristic porosity as well as apparent free energy of adsorption. In linear form, it is expressed as Eq. (7) [35]:

$$\ln q_e = \ln q_m - \left(\beta \varepsilon^2 2\right) \tag{7}$$

$$\varepsilon = RT \ln\left[1 + \frac{1}{C_e}\right] \tag{8}$$

$$E = \frac{1}{\sqrt{\left(-2\beta\right)}} \tag{9}$$

where q_m (mg/g) is the D-R isotherm adsorption capacity, β or K_{ad} (mol^2/kJ^2) is D-R isotherm constant, ε (J/mol) is the Polanyi potential, and E means free adsorption energy. Scatchard adsorption isotherm was applied to investigate the equilibrium behavior of adsorption process. This model was selected to explain metal ions and active side of *Limonia acidissima* shell carbon interaction relationship [36].

$$\frac{q_e}{C_e} = q_m K_b - K_b q_e \tag{10}$$

where q_e (mg/g) represents the adsorbent capacity at equilibrium, q_m (mg/g) is the maximum adsorption capacity, and K_b (L/mg) is Scatchard constant. The plot between q_e/C_e vs. q_e gives the value of q_m and K_b.

2.5. Adsorption kinetic models

The adsorption kinetics can be based on diffusion mass transfer processes or chemical reaction kinetics. There are three different reaction kinetic adsorption models such as pseudo-first-order, pseudo-second-order, and intraparticle diffusion models. These models were applied to analyze the kinetic mechanism by Eqs. (11)–(13), respectively [37].

$$\ln\left(q_e - q_t\right) = \ln q_e - \frac{K_1}{2.303}t \tag{11}$$

$$\frac{t}{q_t} = \left(\frac{1}{K_2 q_e^2} = \frac{1}{q_e t}\right) \tag{12}$$

$$q_t = K_{\text{id}} t^{0.5} + C \tag{13}$$

Here K_1 (min^{-1}) is rate constant first order, K_2 (g mg^{-1} min^{-1}) is pseudo-second–order, and K_{id} (mg g^{-1} min$^{-0.5}$) is intraparticle diffusion; q_e (mg/g) and q_t (mg/g) are adsorption capacity at equilibrium and any time t; C is the intercept.

2.6. Thermodynamic parameters

The thermodynamic parameters conclude whether the adsorption process is spontaneous or not. The thermodynamic parameters such as a change in Gibb's free energy $\Delta G°$, change in enthalpy $\Delta H°$ and change in entropy $\Delta S°$ were calculated using Langmuir isotherm and Van't Hoff equations (represented by Eqs. (14)–(16)), respectively [38];

$$K_c = \frac{C_e}{C_0 - C_e} \tag{14}$$

$$\Delta G° = -RT \ln\left(55.5 \times K_c\right) \tag{15}$$

$$\ln\left(55.5 \times K_c\right) = \left(\frac{\Delta S°}{R} - \frac{\Delta H°}{RT}\right) \tag{16}$$

Here C_0 and C_e are initial concentration and equilibrium concentration of metals ions (mg/g); K_c (L/mg) is Langmuir equilibrium constant; the number 55.5 is the molecular weight of water in 1 L of aqueous solution (dividing 1,000 g/L by 18 g/mol); Universal gas constant R (8.314 J/mol K); T (K) is the temperature. The value of $\Delta H°$ and $\Delta S°$ was obtained with plot ln K_c vs. $1/T$.

3. Result and discussions

3.1. Characterization of *Limonia acidissima* shell carbons

Surface morphology of unmodified *Limonia acidissima* shell, modified *Limonia acidissima* shell, before and after adsorption of As(III) and Cu(II) was examined by scanning electron microscopy in Figs. 1a–d, respectively. In Fig. 1a, unmodified *Limonia acidissima* shell exhibited a dense and some porous surface texture. Large uniform pores are formed on the surface of modified *Limonia acidissima* shell, which shows that H_2SO_4 is effective in developing pores with specific dimensions in *Limonia acidissima* shell carbons. The large pores were covered after contact with As(III) and Cu(II). Interaction with these metals ions the scanning electron microscopy (SEM) analysis clearly represents the rough and irregular surface. The main reason is cross linking between the As(III) and Cu(II) and negatively charged groups such as hydroxyl, carboxyl, etc. in the *Limonia acidissima* shell carbon and confirm the increased surface adsorption of As(III) and Cu(II) [39,40]. The specific surface area of unmodified and modified *Limonia acidissima* shell is 56.68 and 79.67 m^2/g, respectively. The pore volume and pore diameter of unmodified and modified *Limonia acidissima* shell are found to be 0.196 and 0.219 cc/g; and 5.93 and 7.149 nm, respectively.

A Fourier transform infrared spectroscopy (FTIR) in the range 500–4,000 cm^{-1} of unmodified, before adsorption of modified *Limonia acidissima* shell, after adsorption of As(III) and Cu(II) are presented in Table 1. For unmodified *Limonia acidissima* shell carbon, the band at 3,310 cm^{-1} was allocated to O–H stretching and peak at 2,929 cm^{-1} to C–H stretching of alkenes, sharp band across at 1,748 cm^{-1} to C=O stretching carboxylic acids, the band observing at 1,602 cm^{-1} was indicated the C=C stretches of amine group, a band across 1,513 and 1,374 cm^{-1} arises due to N=O stretching group, the band assigned at 1,250 and 1,037 cm^{-1} to aromatic –C–O–C– strong stretching group [41]. The band observed at 550–850 cm^{-1} was assigned to C–Cl strong stretching group. For modified *Limonia acidissima* shell carbon, the stretching free of O–H groups was shifted from 3,310 to 3,709 cm^{-1} after modification of *Limonia acidissima* shell. These results showed that increased water O–H groups after modification of *Limonia acidissima* shell surface. A peak reallocation from 2,929 to 2,944 cm^{-1} is due to aliphatic CH stretching. The band shift from 1,513 to 1,511 cm^{-1} is approximately same, it shows C=C stretching of aromatic functional group. The peak was shifted from 1,037 to 1,052 cm^{-1}. The peaks around 1,748; 1,602; 1,334; 832; and 612 cm^{-1} disappeared after modification of *Limonia acidissima* shell surface. As shown in

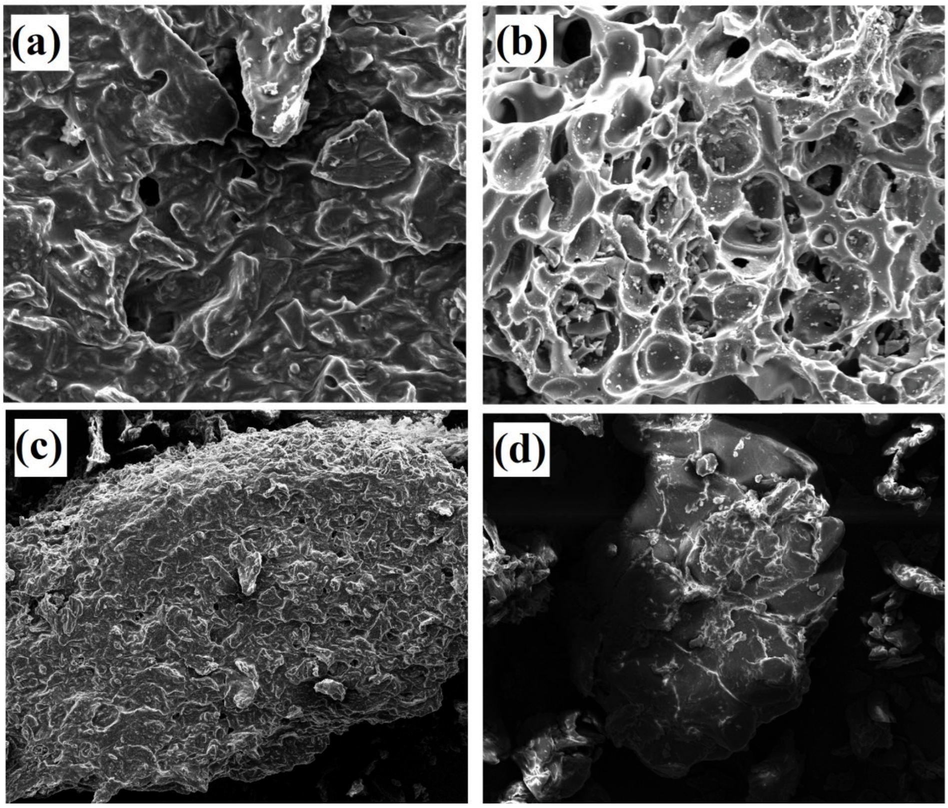

Fig. 1. (a) SEM image (a) unmodified and (b) modified *Limonia acidissima* shell (c) after adsorption of As(III) *Limonia acidissima* shell carbon, and (d) after adsorption of Cu(II) on *Limonia acidissima* shell carbon.

Table 1
FTIR spectrum of (a) unmodified *Limonia acidissima* shell, (b) modified *Limonia acidissima* shell, (c) after adsorption of As(III) and (d) after adsorption of Cu(II)

Functional groups	Peak at unmodified *Limonia acidissima* shell (cm^{-1})	Peak at modified *Limonia acidissima* shell (cm^{-1})	Peak at after adsorption of As(III) (cm^{-1})	Peak at after adsorption of Cu(II) (cm^{-1})
O–H	3,310	3,709	3,678	3,700
C–H	2,929	2,944	3,053; 2,884; 2,825	3,014
C=O	1,748	–	–	–
C=C	1,602	–	–	–
N=O	1,513; 1,374	1,511	1,562	1,562
–C–O–C	1,250; 1,037	1,052	1,253; 996	1,213; 930

Table 1, some peaks apparent shifts from the *Limonia acidissima* shell carbon surface were seen after adsorption of As(III) and Cu(II), respectively. These bands were shifted from 3,709 to 3,670 cm^{-1} and 3,700 cm^{-1} in case of As(III) and Cu(II) adsorption, respectively; from 2,944 to 3,053 cm^{-1}, 2,884 cm^{-1}, and 2,825 cm^{-1} in case of As(III) adsorption and 3,014 cm^{-1} in case of Cu(II) adsorption; the band from 1,511 to 1,562 cm^{-1} for both metals ions adsorption; some new peaks arise (1,253 cm^{-1}) in case of As(III) adsorption and (1,213 cm^{-1}) in case of Cu(II) ions adsorption; from 1,052 to 996 cm^{-1} and 930 cm^{-1} for adsorption of As(III) and Cu(II), respectively [41,42]. In this study, the formation of new absorption band and changes in band frequencies with the energy level of the functional groups could be due to adsorption of As(III) and Cu(II) on *Limonia acidissima* shell carbon surfaces. The active sites of carbon surfaces filled with metals ions due to electrostatic attraction or complexation mechanism (electron pair sharing between electron donor atoms O and N). FTIR spectrum results confirm that the hydroxyl, amine, carboxyl, ester, and carbonate groups are present in active sites of *Limonia acidissima* shell carbon surfaces [43]. The X-ray diffraction (XRD) pattern of *Limonia acidissima* shell carbon is shown in Fig. 2. From the figure, the characteristic diffraction of *Limonia acidissima* shell carbon at around 20°–25° was detected. The diffraction in the spectrum showed no apparent crystalline peak in the 10°–70° scanning range, thus indicating the amorphous phase of *Limonia acidissima* shell carbon.

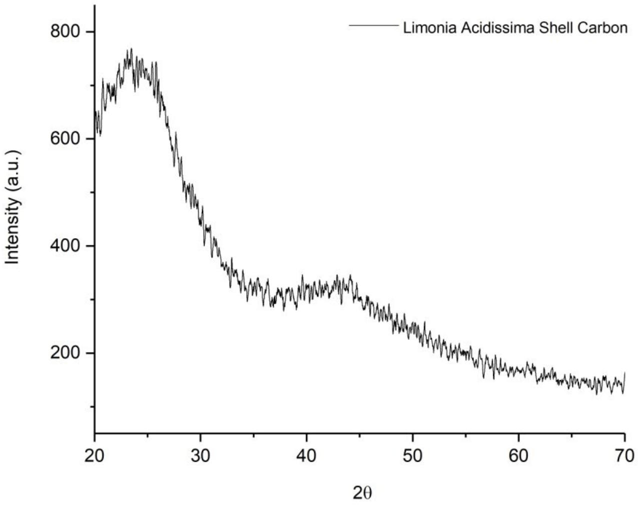

Fig. 2. XRD spectrum of *Limonia acidissima* shell carbon.

3.2. Batch studies

3.2.1. Effect of the initial concentration of As(III) and Cu(II)

Fig. 3a shows the percentage of mg/L of removal and adsorption capacities of As(III) and Cu(II). It can be observed from the figure that the As(III) and Cu(II) elimination rate decreased with the increase of initial concentration, the percentage elimination of As(III) and Cu(II) on *Limonia acidissima* shell carbons decreases from 92.2 to 64.9 for As(III) and 84.6 to 65.3 for Cu(II) as the initial concentration of both the metal ions was increased from 50 to 100 mg/L. At the lower initial concentration of As(III) and Cu(II), the ratio of the available adsorption sites of *Limonia acidissima* shell carbon to the initial number of metals molecules is large, and subsequently, their removal percentage does not get much affected. However, at higher concentration, the available sites of adsorption became fewer, and the percentage removal of As(III) and Cu(II) decreases, which depend upon the initial concentration [33,44,45]. The complete scenario was opposite in terms of adsorption capacity of As(III) and Cu(II) on *Limonia acidissima* shell carbon. The adsorption capacity of As(III) and Cu(II) decreases with increasing the initial concentration of metal ions.

3.2.2. Effect of contact time of As(III) and Cu(II) on *Limonia acidissima* shell carbon

Fig. 3b represents the percentage of removal and adsorption capacities of As(III) and Cu(II) vs. time of contact with heavy metals concentration (50 mg/L) at pH 7. The adsorption rate of As(III) and Cu(II) increases with increase in contact time and achieve saturation in 80 min. In the starting, the adsorption rate of metal ions is fast, but it decreases gradually with time until it reaches equilibrium. At the starting, the percentage of elimination and adsorption capacity is fast due to a larger surface area of the *Limonia acidissima* shell carbons being available for adsorption of both heavy metal ions [45,46].

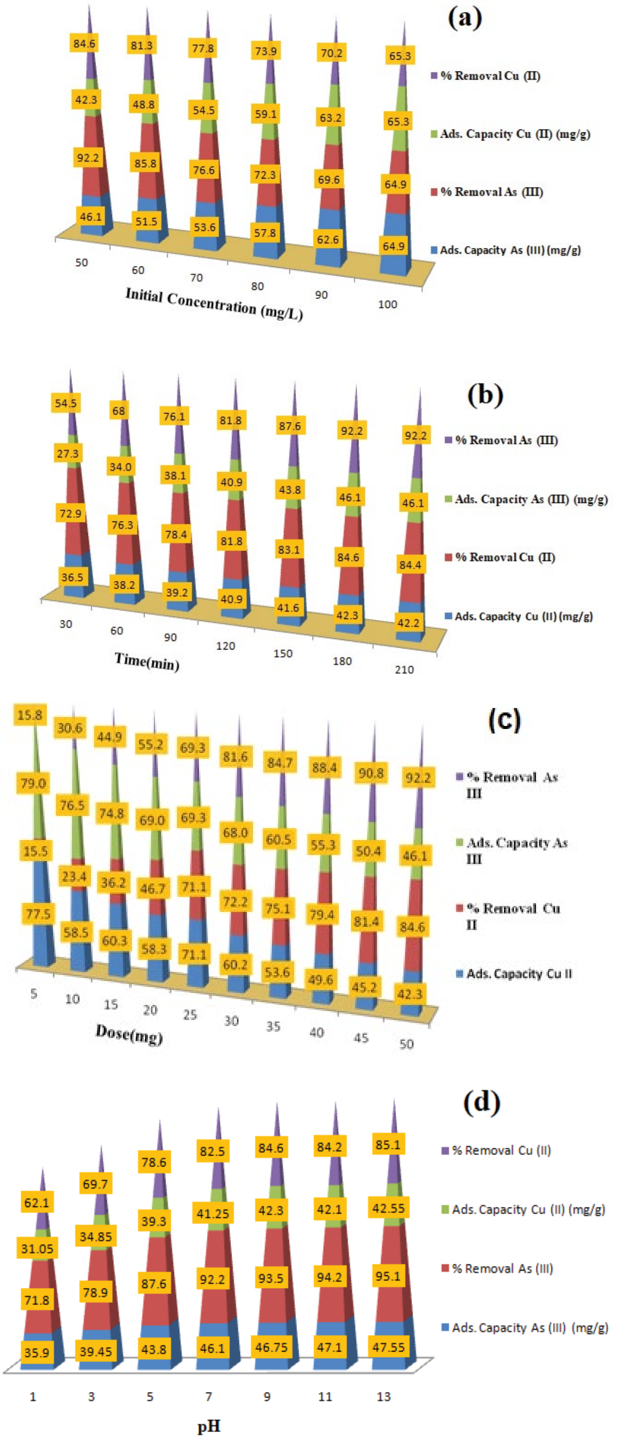

Fig. 3. (a) Effect of initial concentration (contact time = 180 min, temperature = 30°C, adsorbent dosage = 50 mg, pH = 7), (b) effect of contact time of As(III) and Cu(II) on *Limonia acidissima* shell carbon (II) (metals ions concentration = 50 mg/L, temperature = 30°C, adsorbent dosage = 50 mg, pH = 7), (c) effect of *Limonia acidissima* shell carbon dosage on adsorption of As(III) and Cu(II) (initial concentration = 50 mg/L, temperature = 30°C, pH = 7, time = 180 min) and (d) effect of pH (initial concentration = 50 mg/L, adsorbent dosage = 50 mg, temperature = 30°C, time = 180 min).

3.2.3. Effect of adsorbent dosage on adsorption of heavy metals (As(III) and Cu(II))

Effects of adsorbent (*Limonia acidissima* shell carbon) dosage on adsorption of As(III) and Cu(II) are shown in Fig. 3c. The percentage removal of As(III) and Cu(II) increases with the increasing adsorbed amount at fixed metal concentration. It is explained by the greater availability of the active sites or surface area at higher dosages of the adsorbent. The adsorption capacity of As(III) and Cu(II) logically decreased with increasing the dosage of adsorbents because it is directly proportional to the concentration of metal ions in equilibrium (C_e, the concentration of metal ions after adsorption) [47].

3.2.4. Effect of pH

The effect of pH, for percentage removal and adsorption capacity of As(III) and Cu(II) on *Limonia acidissima* shell carbon has been shown in Fig. 3d. This influences the surface charge of activated carbon, speciation of metal ions, and degree of ionization. It can be seen that the percentage removal of As(III) and Cu(II) *Limonia acidissima* shell carbon increased with increasing pH. The maximum percentage removal (92.2 and 84.6) for As(III) and Cu(II) was investigated at pH 7. It was found that the percentage removal of these heavy metals was low at low pH. This might be due to competition between protons and both metal ions for active adsorption sites. *Limonia acidissima* shell carbon surface became more negatively charged when pH was varied from 1 to 13. The functional groups got deprotonated which made adsorption of As(III) and Cu(II) ions competitive. However, when the pH of the solution is high, the higher adsorption of both the metal ions was observed due to combination of adsorption and precipitation.

3.3. Adsorption isotherm models

Several models have been used in the literature to describe the experimental data of adsorption isotherms. In the present work, Langmuir, Freundlich, Temkin, D-R, and Scatchard isotherm models were used. Figs. 4a–d represent the Langmuir, Freundlich, Temkin, and D-R isotherm models. The adsorption constants, correlations coefficients, and other parameters for As(III) and Cu(II) onto *Limonia acidissima* carbons obtained from Langmuir (Eqs. (3) and (4), Freundlich (Eq. (5)), Temkin (Eq. (6)), D-R isotherm (Eqs. (7)–(9)), and Scatchard (Eq. (10)) models are given in Table 2. Correlation coefficients suggested that the Langmuir isotherm model for both metals was the best fit than the Freundlich, Temkin, and D-R isotherm (R^2 = 0.9910 and 0.9996 for As(III) and Cu(II), respectively). The maximum adsorption capacities of *Limonia acidissima* carbons for As(III) and Cu(II) (68.77 and 76.92 mg/g, respectively) were obtained. The parameter K_L is related to the affinity of the binding sites, *Limonia acidissima* shell carbon had a higher affinity (0.3267 L/mg) for As(III) than Cu(II) (0.1533 L/mg). The separation factor (R_L) values 0.0576 and 01153 calculated from Eq. (4) in the range 0–1 indicated the favorable adsorption of As(III) and Cu(II) on *Limonia acidissima* shell carbon [46]. From Fig. 4d, the value K_{ad} was calculated to be 0.829×10^{-6} and 4.715×10^{-6} for As(III)

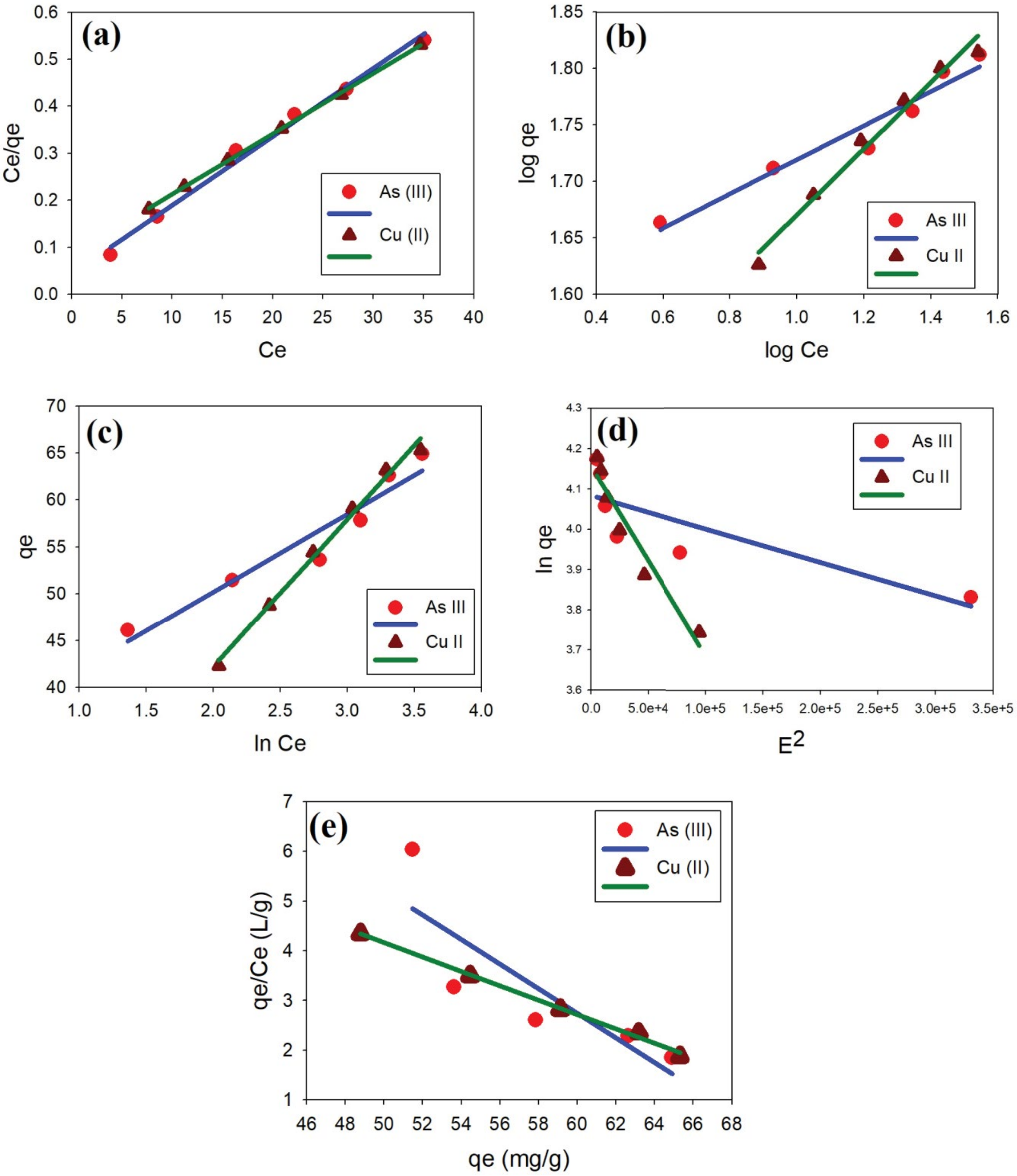

Fig. 4. (a) Langmuir adsorption isotherm, (b) Freundlich adsorption isotherm, (c) Temkin adsorption isotherm and (d) D-R adsorption isotherm for adsorption of As(III) and Cu(II) onto *Limonia acidissima* shell carbon and (e) Scatchard isotherm plot (contact time = 180 min, temperature = 30°C, adsorbent dosage = 50 mg, pH = 7).

and Cu(II) adsorption, respectively. The mean free energy, *E*, plays an important role to know the nature of adsorption, which is either physical or chemical adsorption. If the value of *E* is lower than 8 kJ/mol, physical adsorption dominates, and if the value of *E* is in range 8–16 kJ/mol, the adsorption process explained the chemical adsorption. The mean free energy (*E*) was determined to be 0.7765 and 0.325 kJ/mol for As(III) and Cu(II), showing physisorption [48–50]. Scatchard constant (K_b) for As(III) (0.2470) and Cu(II) (0.1447) and maximum adsorption capacity 71.10 mg/g for As(III) and 78.83 mg/g for Cu(II) were obtained by Eq. (10). In Fig. 4e, the deviation from linear curve illustrates the presence of more than one nature of active sites of the adsorption of metals ions on *Limonia acidissima* shell carbon, although the Scatchard plot is linear, it indicates that vacant active sites are identical and independent [51,52].

3.4. Adsorption kinetic models

The linear form of pseudo-first-order, pseudo-second-order adsorption kinetic models and intraparticle diffusion of heavy metals (As(III) and Cu(II)) adsorbed on the *Limonia acidissima* carbon are shown in Figs. 5a–c, respectively and their computed parameters are presented in Table 3. It can be observed from Table 3 that the correlation coefficients (R^2) values were higher (viz. 0.9974 and 0.9994 for As(III) and Cu(II), respectively) for the pseudo-second-order kinetic model, which suggests that the adsorption process is caused

Table 2
Langmuir, Freundlich, Temkin, and Dubinin–Radushkevich isotherm constants for the adsorption of As(III) and Cu(II) onto *Limonia acidissima* shell carbon

Model		As(III)	Cu(II)
Langmuir	q_m (mg/g)	68.77	76.92
	K_L (L/mg)	0.3267	0.1533
	R_L	0.0576	0.1153
	R^2	0.9910	0.9996
Freundlich	$1/n$	0.1513	0.2932
	n	6.6079	3.4095
	K_F (mg/g)	4.2618	3.7433
	R^2	0.9433	0.9811
Temkin	A_T (L/mg)	11.0588	1.8815
	b_T	304.30	160.54
	B (J/mol)	8.2748	15.6916
	R^2	0.9226	0.9923
Dubinin–Radushkevich	q_m (mg/g)	11.0998	11.3010
	K_{ad} (mol²/kJ²)	0.829×10^{-6}	4.715×10^{-6}
	E (kJ/mol)	0.7765	0.325
	R^2	0.6825	0.9360
Scatchard	q_m (mg/g)	71.10	78.83
	K_b (L/mg)	0.2470	0.1447
	R^2	0.7199	0.9960

by chemisorptions. Chemisorptions (chemical reaction) process involved the valance forces resulting from electron sharing between metal ions and *Limonia acidissima* shell carbon where the metals ions are attached to the *Limonia acidissima* shell carbon surface by chemical bonds [53–57]. The intraparticle diffusion parameters from Table 3 show that the adsorption process is complex and involves more than one mechanism. From Fig. 5c (plots q_t vs. $t^{0.5}$) indicates that if a straight line passes through the origin, adsorption process is controlled by intraparticle diffusion, while if a straight line does not pass through the origin, the adsorption process is controlled by more than another mechanism [38,58].

3.5. Thermodynamic parameters study

Thermodynamic parameters during adsorption of As(III) and Cu(II) on *Limonia acidissima* shell carbon were calculated from Eqs. (14)–(16) on a temperature range of 293 to 333 K from the slope and intercept of Fig. 5d. The values of these parameters are represented in Table 4. Adsorption of As(III) and Cu(II) on *Limonia acidissima* shell carbon increases with increase of temperature; this shows that the adsorption was an endothermic process. The positive value of enthalpy change shows that the adsorption is also an endothermic process. The negative value of Gibb's free energy shows that the adsorption was a spontaneous process. A comparative study is shown in Table 5 for the removal of As(III) and Cu(II) by different activating carbon materials reported in the literature.

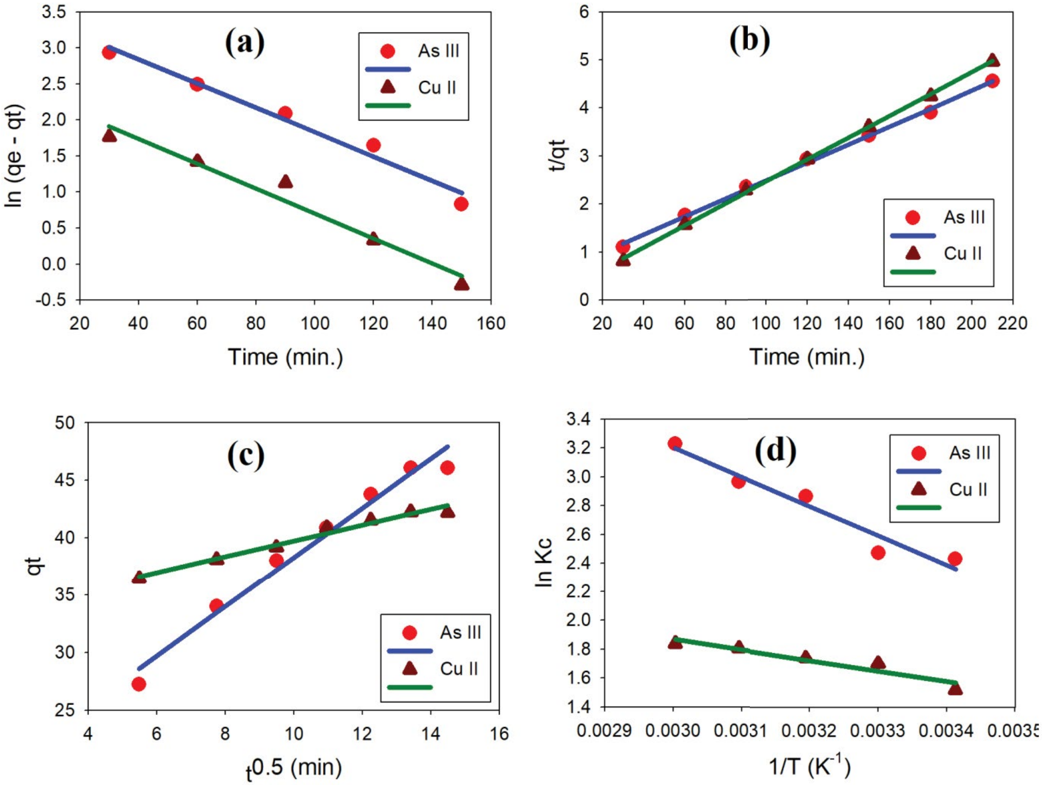

Fig. 5. (a) Pseudo-first-order plot, (b) pseudo-second-order plot, (c) intra-particle-diffusion plot, and (d) Van't Hoff plot for adsorption of As(III) and Cu(II) onto *Limonia acidissima* shell carbons (metals ions concentration = 50 mg/L, temperature = 30°C, adsorbent dosage = 50 mg, pH = 7).

Table 3
Summary of parameters for various adsorption kinetic models for As(III) and Cu(II) on *Limonia acidissima* shell carbon

Kinetic model	Parameter	As(III)	Cu(II)
Pseudo-first-order	q_e (mg/g)	11.4313	6.6097
	K_1 (min)$^{-1}$	0.0168	0.0173
	R^2	0.9765	0.9627
Pseudo-second-order	q_e(mg/g)	53.4956	43.8881
	K_2 (g/mg min)	0.00056	0.0027
	R^2	0.9974	0.9994
Intra-particle diffusion	K_{id} (g/mg min$^{0.5}$)	2.1439	0.6872
	C (mg/g)	16.8475	32.8609
	R^2	0.9752	0.9722

Table 4
Summary of thermodynamic parameters for As(III) and Cu(II) on *Limonia acidissima* shell carbon

Thermodynamic parameters	As(III)	Cu(II)
$\Delta H°$ (kJ/mol)	16.986	6.052
$\Delta S°$ (J/mol K)	110.931	67.044
R^2	0.9451	0.9047
$-\Delta G°$ (kJ/mol)		
293 (K)	15.699	13.478
303 (K)	16.322	14.393
313 (K)	17.886	14.969
323 (K)	18.732	15.627
333 (K)	20.048	16.197

Table 5
Comparison between adsorption capacity of numerous activated carbons for As(III) and Cu(II) from single solutions

Adsorbents	q_e (mg/g)		References
	As(III)	Cu(II)	
Sacebarmyces cerevisiae	0.11	–	[59]
Unmodified iron ore sludge	1.113	–	[60]
Activated carbons from solvent extracted olive pulp	1.393	–	[61]
GAC treated with $FeCl_2$	2.0	–	[62]
Fe-Mn-modified granular activated carbon	2.87	–	[63]
Oak wood char	5.85	–	[64]
Oak bark char	7.40	–	[64]
Pine bark char	12.15	–	[64]
Fe-Mn-La-impregnated biochar	15.34	–	[65]
Water hyacinth	–	2.06	[66]
Magnetic biochar derived from water hyacinth	–	3.53	[66]
Hardwood char	–	6.79	[17]
Corn straw char	–	12.52	[17]
Lime sand bricks	–	7 ± 1	[67]
Coconut coir dust	–	7.463	[68]
Sugarcane bagasse treated with HCl	–	16.98	[69]
Sugarcane bagasse treated with NaOH	–	24.57	[69]
Chitosan-SP/PET composite	–	34.8	[70]
AC impregnated iron oxide	32.86	–	[71]
Iron modified activated carbon	39.2	–	[72]
ZrPACM-43 hybrid material	41.49	–	[73]
Limonia acidissima shell carbons	68.77	76.92	Present material

4. Conclusion

In this study, the kinetics of As(III) and Cu(II) adsorption onto activated carbon prepared from *Limonia acidissima* shell was examined. The effect of various parameters, such as initial concentration, adsorbent dosage, and contact time, were determined. The process optimization of mentioned parameters was also intended and best conditions 50 mg of *Limonia acidissima* shell carbon at 303 K with 180 min, 92.2% and 84.1% of As(III) and Cu(II) removal was achieved. The equilibrium data were analyzed using various adsorption isotherm models. The best-fitted isotherm was Langmuir isotherm model for As(III) and Cu(II). The adsorption process best fit into the pseudo-second-order kinetic model for both the heavy metals on activated carbon prepared from *Limonia acidissima* shell. The thermodynamic studies indicated that the adsorption requires a low amount of energy to start, is spontaneous and is endothermic in nature. *Limonia acidissima* shell carbon was found to exhibit higher capacities for the elimination of As(III) and Cu(II) than other activating carbon materials reported in the literature.

Acknowledgments

The authors are grateful to the University Grant Commission (UGC-RGNFD) [F/2014-15/RGNF-2014-15D-OBC-HAR-59079], for providing financial support.

References

[1] C.T. Kamala, K.H. Chu, N.S. Chary, P.K. Pandey, S.L. Ramesh, A.R.K. Sastry, K.C. Sekhar, Removal of arsenic (III) from aqueous solutions using fresh and immobilized plant biomass, Water Res., 39 (2005) 2815–2826.

[2] Ö. Gerçel, H.F. Gerçel, Adsorption of lead(II) ions from aqueous solutions by activated carbon prepared from biomass plant material of *Euphorbia rigida*, Chem. Eng. J., 132 (2007) 289–297.

[3] M.A. Barakat, New trends in removing heavy metals from industrial wastewater, Arab. J. Chem., 4 (2011) 361–377.

[4] O.E. Abdel Salam, N.A. Reiad, M.M. ElShafei, A study of the removal characteristics of heavy metals from wastewater by low-cost adsorbents, J. Adv. Res., 2 (2011) 297–303.

[5] C. Namasivayam, K. Ranganathan, Removal of Pb (II), Cd (II), Ni (II) and Mixture of Metal Ions by Adsorption onto ' Waste ' Fe (III)/ Cr (III) Hydroxide and Fixed Bed Studies, Environ. Technol., 16 (2010) 851–860.

[6] B.E. Susan, O.J. Trudy, R.M. Bricka, D.D. Adrian, A review of potentially low-cost sorbents for heavy metals, Water Res., 33 (1999) 2469–1999.

[7] J.C. Igwe, D.N. Ogunewe, A.A. Abia, Competitive adsorption of Zn (II), Cd (II) AND Pb (II) ions from aqueous and non- aqueous solution by maize cob and husk, African J. Biotechnol., 4 (2005) 1113–1116.

[8] M. Ajmal, R. Ali, K. Rao, R. Ahmad, J. Ahmad, Adsorption studies on *Citrus reticulata* ž fruit peel of orange / : removal and recovery of Ni ž II / from electroplating wastewater, J. Hazard Mater., 79 (2000) 117–131.

[9] R.R. Bansode, J.N. Losso, W.E. Marshall, R.M. Rao, R.J. Portier, Adsorption of metal ions by pecan shell-based granular activated carbons, Bioresour. Technol., 89 (2003) 115–119.

[10] N.R. Bishnoi, M. Bajaj, N. Sharma, A. Gupta, Adsorption of Cr (VI) on activated rice husk carbon and activated alumina, Bioresour. Technol., 91 (2004) 305–307.

[11] S. Babel, T.A. Kurniawan, Cr (VI) removal from synthetic wastewater using coconut shell charcoal and commercial activated carbon modified with oxidizing agents and / or chitosan, Chemosphere, 54 (2004) 951–967.

[12] P.L. Tang, C.K. Lee, K.S. Low, Z. Zainal, Sorption of Cr (VI) and Cu (II) in aqueous solution by ethylenediamine modified rce hull, Environ. Technol., 24 (2012) 1243–1251.

[13] M. Momcilovic, M. Purenovi, A. Boji, A. Zarubica, M. Ran, Removal of lead (II) ions from aqueous solutions by adsorption onto pine cone activated carbon, Desalination, 276 (2011) 53–59.

[14] E. Demirbas, N. Dizge, M.T. Sulak, M. Kobya, Adsorption kinetics and equilibrium of copper from aqueous solutions using hazelnut shell activated carbon, Chem. Eng. J., 148 (2009) 480–487.

[15] M.I. Sabela, K. Kunene, S. Kanchi, N.M. Xhakaza, A. Bathinapatla, P. Mdluli, D. Sharma, K. Bisetty, Removal of copper (II) from wastewater using green vegetable waste derived activated carbon: an approach to equilibrium and kinetic study, Arab. J. Chem., 12 (2019) 4331–4339

[16] M.M. Rao, D.K. Ramana, K. Seshaiah, M.C. Wang, S.W.C. Chien, Removal of some metal ions by activated carbon prepared from *Phaseolus aureus* hulls, J. Hazard. Mater., 166 (2009) 1006–1013.

[17] X. Chen, G. Chen, L. Chen, Y. Chen, J. Lehmann, M.B. Mcbride, A.G. Hay, Adsorption of copper and zinc by biochars produced from pyrolysis of hardwood and corn straw in aqueous solution, Bioresour. Technol., 102 (2011) 8877–8884.

[18] L. Wang, J. Zhang, R. Zhao, Y. Li, C. Li, C. Zhang, Adsorption of Pb (II) on activated carbon prepared from *Polygonum orientale* Linn.: kinetics, isotherms, pH, and ionic strength studies, Bioresour. Technol., 101 (2010) 5808–5814.

[19] M. Valix, W.H. Cheung, K. Zhang, Role of heteroatoms in activated carbon for removal of hexavalent chromium from wastewaters, J. Hazard. Mater., 135 (2006) 395–405.

[20] G. Mahajan, D. Sud, Modified agricultural waste biomass with enhanced responsive properties for metal-ion remediation : a green approach, Appl. Water Sci., 2 (2012) 299–308.

[21] V. Sarin, K.K. Pant, Removal of chromium from industrial waste by using eucalyptus bark, Bioresour. Technol., 97 (2006) 15–20.

[22] H. Jalayeri, F. Pepe, Novel and high-performance biochar derived from pistachio green hull biomass: production, characterization, and application to Cu(II) removal from aqueous solutions, Ecotoxicol. Environ. Saf., 168 (2019) 64–71.

[23] J. Acharya, U. Kumar, B.C. Meikap, Thermodynamic spectral and kinetic analysis of the removal of Cu(II) from aqueous solution by sodium carbonate treated rice husk, J. Environ. Sci. Health Part A, 54 (2019) 1–9.

[24] M. Manjuladevi, R. Anitha, S. Manonmani, Kinetic study on adsorption of Cr(VI), Ni(II), Cd(II) and Pb(II) ions from aqueous solutions using activated carbon prepared from *Cucumis melo* peel, Appl. Water Sci., 8 (2018) 1–8.

[25] V. Yadav, D.P. Tiwari, M. Bhagat, Arsenic removal using chemically modified *Kigelia africana* as a low-cost bio- adsorbent: equilibrium, kinetics and thermodynamics studies, Int. J. Basic Appl. Res., 9 (2019) 1282–1294.

[26] G.V.S.R. Pavan Kumar, K.A. Malla, B. Yerra, K. Srinivasa Rao, Removal of Cu(II) using three low-cost adsorbents and prediction of adsorption using artificial neural networks, Appl. Water Sci., 9 (2019) 1–9.

[27] H.S. Mohamed, N.K. Soliman, D.A. Abdelrheem, A.A. Ramadan, A.H. Elghandour, S.A. Ahmed, Adsorption of Cd^{2+} and Cr^{3+} ions from aqueous solutions by using residue of *Padina gymnospora* waste as promising low-cost adsorbent, Heliyon, 5 (2019) e01287.

[28] J. Guo, W. Sheng, Y. Lin, A. Chong, Adsorption of NH_3 onto activated carbon prepared from palm shells impregnated with H_2SO_4, J. Colloid Interface Sci., 281 (2005) 285–290.

[29] F.S. Mohamed, W.A. Khater, M.R. Mostafa, Characterization and phenols sorptive properties of carbons activated by sulphuric acid, Chem. Eng. J., 116 (2006) 47–52.

[30] C. Suresh, D.H.K. Reddy, Y. Harinath, B.R. Naik, K. Seshaiah, A.V.R. Reddy, Development of wood apple shell (*Feronia acidissima*) powder biosorbent and its application for the removal of Cd(II) from aqueous solution, Sci. World J., 2014 (2014) 1–8.

[31] D.M. Kailas, K.M. Ejazuddin, Equilibrium, kinetics and diffusion mechanism of Cr (VI) adsorption onto activated carbon derived from wood apple shell, Arab. J. Chem., 10 (2017) 252–260.

[32] S. Dawood, T.K. Sen, C. Phan, Synthesis and characterisation of novel-activated carbon from waste biomass pine cone and its application in the removal of congo red dye from aqueous solution by adsorption, Water. Air. Soil Pollut., 225 (2014) 1818–1834.

[33] U. Osman, G. Unal, K. Hakan, B. Yuksel, Adsorptive removal of Rhodamine B with activated carbon obtained from Okra Wastes, Chem. Eng. Commun., 204 (2017) 772–783.

[34] V. Yadav, P. Kumar, D.P. Tiwari, M. Bhagat, 62%SiO_2-32%CaO-6%P_2O_5 bioglass as adsorbent for the removal of Congo red dye, Int. J. Eng. Technol. Sci. Res., 4 (2017) 364–369.

[35] R. Laus, T.G. Costa, B. Szpoganicz, V.T. Fávere, Adsorption and desorption of Cu(II), Cd(II) and Pb(II) ions using chitosan crosslinked with epichlorohydrin-triphosphate as the adsorbent, J. Hazard. Mater., 183 (2010) 233–241.

[36] M. Shafiee, R. Foroutan, K. Fouladi, M. Ahmadlouydarab, B. Ramavandi, S. Sahebi, Application of oak powder/Fe_3O_4 magnetic composite in toxic metals removal from aqueous solutions, Adv. Powder Technol., 30 (2019) 544–554.

[37] R.M.M. dos Santos, R.G.L. Gonçalves, V.R.L. Constantino, C.V. Santilli, P.D. Borges, J. Tronto, F.G. Pinto, Adsorption of Acid Yellow 42 dye on calcined layered double hydroxide: effect of time, concentration, pH and temperature, Appl. Clay Sci., 140 (2017) 132–139.

[38] H.N. Tran, S.J. You, H.P. Chao, Thermodynamic parameters of cadmium adsorption onto orange peel calculated from various methods: a comparison study, J. Environ. Chem. Eng., 4 (2016) 2671–2682.

[39] N. Feng, X. Guo, Liang sha, adsorption study of copper (II) by chemically modified orange peel, J. Hazard. Mater., 164 (2009) 1286–1292.

[40] A. Florido, C. Valderrama, J.A. Arévalo, I. Casas, M. Martínez, N. Miralles, Application of two sites non-equilibrium sorption model for the removal of Cu(II) onto grape stalk wastes in a fixed-bed column, Chem. Eng. J., 156 (2010) 298–304.

[41] V. Yadav, D.P. Tiwari, M. Bhagat, Activated Carbon of *Kigelia africana* as bio-adsorbent: synthesis and characterization, Int. J. Res. Anal. Rev., 6 (2019) 958–964.

[42] Ş. Parlayici, E. Pehlivan, Comparative study of Cr(VI) removal by bio-waste adsorbents: equilibrium, kinetics, and thermodynamic, J. Anal. Sci. Technol., 10 (2019) 1–8.

[43] W. Pranata Putra, A. Kamari, S. Najiah Mohd Yusoff, C. Fauziah Ishak, A. Mohamed, N. Hashim, I. Md Isa, Biosorption of Cu(II), Pb(II) and Zn(II) ions from aqueous solutions using selected Waste materials: adsorption and characterisation studies, J. Encapsulation Adsorpt. Sci., 4 (2014) 25–35.

[44] S. Yao, S. Sun, S. Wang, Z. Shi, Adsorptive removal of lead ion from aqueous solution by activated carbon/iron oxide magnetic composite, Indian J. Chem. Technol., 23 (2016) 146–152.

[45] L.J. Yu, S.S. Shukla, K.L. Dorris, A. Shukla, J.L. Margrave, Adsorption of chromium from aqueous solutions by maple sawdust, J. Hazard. Mater., 100 (2003) 53–63.

[46] V. Yadav, Tiwari, D.P.M. Bhagat, Removal of Congo Red dye from aqueous solution by using *Limonia acidissima* shell as adsorbent, Asian J. Chem., 30 (2018) 2765–2770.

[47] J. Ndi Nsami, J. Ketcha Mbadcam, The adsorption efficiency of chemically prepared activated carbon from cola nut shells by $ZnCl_2$ on methylene blue, J. Chem., 2013 (2013) 1–3.

[48] A. Dada, A. Olalekan, A. Olatunya, O. DADA, Langmuir, Freundlich, Temkin and Dubinin–Radushkevich isotherms studies of equilibrium sorption of Zn^{2+} unto phosphoric acid modified rice husk, IOSR J. Appl. Chem., 3 (2012) 38–45.

[49] A. N, A. T. Ekubo, D.Wankasi, E.D. Dikio, Adsorption of congo red by Ni/Al-CO_3: equilibrium, thermodynamic and kinetic studies, Orient. J. Chem., 31 (2015) 1307–1318.

[50] S.A. Olawale, A.W. Funke, A.H. Dede, A. Habeeb, Isotherm studies of the biosorption of Pb (II) and Cu (II) using chicken feather, Asian J. Adv. Res. Rep., 1 (2018) 1–9.

[51] M. Küçükosmanoğlu, O. Gezici, A. Ayar, The adsorption behaviors of Methylene Blue and Methyl Orange in a diaminoethane sporopollenin-mediated column system, Sep. Purif. Technol., 52 (2006) 280–287.

[52] H. Dumrul, A.N. Kursunlu, O. Kocyigit, E. Guler, S. Ertul, Adsorptive removal of Cu(II) and Ni(II) ions from aqueous media by chemical immobilization of three different aldehydes, Desalination, 271 (2011) 92–99.

[53] Z. Harrache, M. Abbas, T. Aksil, M. Trari, Thermodynamic and kinetics studies on adsorption of Indigo Carmine from aqueous solution by activated carbon, Microchem. J., 144 (2019) 180–189.

[54] A. Sari, M. Tuzen, Kinetic and equilibrium studies of biosorption of Pb(II) and Cd(II) from aqueous solution by macrofungus (*Amanita rubescens*) biomass, J. Hazard. Mater., 164 (2009) 1004–1011.

[55] H. Esmaeili, R. Foroutan, Adsorptive behavior of methylene blue onto sawdust of sour lemon, date palm, and eucalyptus as agricultural wastes, J. Dispers. Sci. Technol., 40 (2019) 990–999.

[56] R. Foroutan, R. Mohammadi, S. Farjadfard, H. Esmaeili, M. Saberi, S. Sahebi, S. Dobaradaran, B. Ramavandi, Characteristics and performance of Cd, Ni, and Pb bio-adsorption using *Callinectes sapidus* biomass: real wastewater treatment, Environ. Sci. Pollut. Res., 26 (2019) 6336–6347.

[57] N. Behrouz, F. Rauf, A. Bahram, R. Farzaneh, S. Bahman, Pb(II) and Cd(II) removal from aqueous solution, shipyard wastewater, and landfill leachate by modified rhizopus oryzae biomass, Mater. Res. Express, 5 (2018) 0–30.

[58] K.C. Bedin, A.C. Martins, A.L. Cazetta, O. Pezoti, V.C. Almeida, KOH-activated carbon prepared from sucrose spherical carbon: adsorption equilibrium, kinetic and thermodynamic studies for Methylene Blue removal, Chem. Eng. J., 286 (2016) 476–484.

[59] B. Mohebbrad, Z. Bonyadi, A.A. Dehghan, M.H. Rahmat, Arsenic removal from aqueous solutions using Saccharomyces cerevisiae: kinetic and equilibrium study, Environ. Prog. Sustain. Energy, 38 (2019) 398–402.

[60] K.M. Nguyen, B.Q. Nguyen, H.T. Nguyen, H.T.H. Nguyen, Adsorption of arsenic and heavy metals from solutions by unmodified iron-ore sludge, Appl. Sci., 619 (2019) 1–14.

[61] T. Budinova, N. Petrov, M. Razvigorova, J. Parra, P. Galiatsatou, Removal of arsenic (III) from aqueous solution by activated carbons prepared from solvent extracted olive pulp and olive stones, Ind. Eng. Chem. Resour., 45 (2006) 1896–1901.

[62] Q. Chang, W. Lin, W. Ying, Preparation of iron-impregnated granular activated carbon for arsenic removal from drinking water, J. Hazard. Mater., 184 (2010) 515–522.

[63] J. Nikić, J. Agbaba, M.A. Watson, A. Tubić, M. Šolić, S. Maletić, B. Dalmacija, Arsenic adsorption on Fe–Mn modified granular activated carbon (GAC–FeMn): batch and fixed-bed column studies, J. Environ. Sci. Health Part A, 54 (2019) 168–178.

[64] D. Mohan, C.U. Pittman, M. Bricka, F. Smith, B. Yancey, Sorption of arsenic, cadmium, and lead by chars produced from fast pyrolysis of wood and bark during bio-oil production, J. Colloid Interface Sci., 310 (2007) 57–73.

[65] L. Lin, G. Zhang, X. Liu, Z.H. Khan, W. Qiu, Z. Song, Synthesis and adsorption of Fe–Mn–La-impregnated biochar composite as an adsorbent for As(III) removal from aqueous solutions, Environ. Pollut., 247 (2019) 128–135

[66] B.C. Nyamunda, T. Chivhanga, U. Guyo, F. Chigondo, Removal of Zn (II) and Cu (II) ions from industrial wastewaters using magnetic biochar derived from water hyacinth, J. Eng. (USA), 2019 (2019) 1–11.

[67] X. Zhang, S. Guo, J. Liu, Z. Zhang, K. Song, C. Tan, H. Li, A study on the removal of copper (II) from aqueous solution using lime sand bricks, Appl. Sci., 9 (2019) 670.

[68] R.E. Ogali, O. Akaranta, I.B. Obot, Removal of Cu (II) from aqueous solution using coconut (*Cocos nucifera* L.) coir dust, Sch. Res. Libr., 2 (2010) 60–75.

[69] M. Tchoumou, C.G. Mananga, C.P.B. Malongo, Removal of copper (II) and nickel (II) from aqueous solution by adsorption on sugarcane bagasse, Int. Res. J. Environ. Sci., 4 (2015) 62–67.

[70] Y. Song, A. Kong, Y. Ji, B. He, H. Wang, J. Li, Adsorption for copper(II) ion with chitosan-SP/PET composite adsorbent enhanced by electric field, Adsorpt. Sci. Technol., 37 (2019) 274–287.

[71] E.A. Deliyanni, G.Z. Kyzas, K.S. Triantafyllidis, K.A. Matis, Activated carbons for the removal of heavy metal ions : a systematic review of recent literature focused on lead and arsenic ions, Open Chem., 13 (2015) 699–708.

[72] W. Chen, R. Parette, J. Zou, F.S. Cannon, B.A. Dempsey, Arsenic removal by iron-modified activated carbon, Water Res., 41 (2007) 1851–1858.

[73] S. Mandal, M.K. Sahu, R. Kishore, Adsorption studies of arsenic (III) removal from water by zirconium polyacrylamide hybrid material (ZrPACM-43), Water Resour. Ind., 4 (2013) 51–67.